

Observation of $D^+ \rightarrow K_S^0 a_0(980)^+$ in the amplitude analysis of $D^+ \rightarrow K_S^0 \pi^+ \eta$

- M. Ablikim¹, M. N. Achasov^{4,b}, P. Adlarson⁷⁵, X. C. Ai⁸¹, R. Aliberti³⁵, A. Amoroso^{74A,74C}, M. R. An³⁹, Q. An^{71,58}, Y. Bai⁵⁷, O. Bakina³⁶, I. Balossino^{29A}, Y. Ban^{46,g}, H.-R. Bao⁶³, V. Batozskaya^{1,44}, K. Begzsuren³², N. Berger³⁵, M. Berlowski⁴⁴, M. Bertani^{28A}, D. Bettoni^{29A}, F. Bianchi^{74A,74C}, E. Bianco^{74A,74C}, A. Bortone^{74A,74C}, I. Boyko³⁶, R. A. Briere⁵, A. Brueggemann⁶⁸, H. Cai⁷⁶, X. Cai^{1,58}, A. Calcaterra^{28A}, G. F. Cao^{1,63}, N. Cao^{1,63}, S. A. Cetin^{62A}, J. F. Chang^{1,58}, T. T. Chang⁷⁷, W. L. Chang^{1,63}, G. R. Che⁴³, G. Chelkov^{36,a}, C. Chen⁴³, Chao Chen⁵⁵, G. Chen¹, H. S. Chen^{1,63}, M. L. Chen^{1,58,63}, S. J. Chen⁴², S. L. Chen⁴⁵, S. M. Chen⁶¹, T. Chen^{1,63}, X. R. Chen^{31,63}, X. T. Chen^{1,63}, Y. B. Chen^{1,58}, Y. Q. Chen³⁴, Z. J. Chen^{25,h}, S. K. Choi¹⁰, X. Chu⁴³, G. Cibinetto^{29A}, S. C. Coen³, F. Cossio^{74C}, J. J. Cui⁵⁰, H. L. Dai^{1,58}, J. P. Dai⁷⁹, A. Dbeysi¹⁸, R. E. de Boer³, D. Dedovich³⁶, Z. Y. Deng¹, A. Denig³⁵, I. Denysenko³⁶, M. Destefanis^{74A,74C}, F. De Mori^{74A,74C}, B. Ding^{66,1}, X. X. Ding^{46,g}, Y. Ding⁴⁰, Y. Ding³⁴, J. Dong^{1,58}, L. Y. Dong^{1,63}, M. Y. Dong^{1,58,63}, X. Dong⁷⁶, M. C. Du¹, S. X. Du⁸¹, Z. H. Duan⁴², P. Egorov^{36,a}, Y. H. Fan⁴⁵, J. Fang^{1,58}, S. S. Fang^{1,63}, W. X. Fang¹, Y. Fang¹, Y. Q. Fang^{1,58}, R. Farinelli^{29A}, L. Fava^{74B,74C}, F. Feldbauer³, G. Felici^{28A}, C. Q. Feng^{71,58}, J. H. Feng⁵⁰, Y. T. Feng⁷¹, K. Fischer⁶⁹, M. Fritsch³, C. D. Fu¹, J. L. Fu⁶³, Y. W. Fu¹, H. Gao⁶³, Y. N. Gao^{46,g}, Yang Gao^{71,58}, S. Garbolino^{74C}, I. Garzia^{29A,29B}, P. T. Ge⁷⁶, Z. W. Ge⁴², C. Geng⁵⁹, E. M. Gersabeck⁶⁷, A. Gilman⁶⁹, K. Goetzen¹³, L. Gong⁴⁰, W. X. Gong^{1,58}, W. Gradi³⁵, S. Gramigna^{29A,29B}, M. Greco^{74A,74C}, M. H. Gu^{1,58}, Y. T. Gu¹⁵, C. Y. Guan^{1,63}, Z. L. Guan²², A. Q. Guo^{31,63}, L. B. Guo⁴¹, M. J. Guo⁵⁰, R. P. Guo⁴⁹, Y. P. Guo^{12,f}, A. Guskov^{36,a}, J. Gutierrez²⁷, T. T. Han¹, W. Y. Han³⁹, X. Q. Hao¹⁹, F. A. Harris⁶⁵, K. K. He⁵⁵, K. L. He^{1,63}, F. H. H. Heinsius³, C. H. Heinz³⁵, Y. K. Heng^{1,58,63}, C. Herold⁶⁰, T. Holtmann³, P. C. Hong^{12,f}, G. Y. Hou^{1,63}, X. T. Hou^{1,63}, Y. R. Hou⁶³, Z. L. Hou¹, B. Y. Hu⁵⁹, H. M. Hu^{1,63}, J. F. Hu^{56,i}, T. Hu^{1,58,63}, Y. Hu¹, G. S. Huang^{71,58}, K. X. Huang⁵⁹, L. Q. Huang^{31,63}, X. T. Huang⁵⁰, Y. P. Huang¹, T. Hussain⁷³, N. Hüsken^{27,35}, N. in der Wiesche⁶⁸, M. Irshad^{71,58}, J. Jackson²⁷, S. Jaeger³, S. Janchiv³², J. H. Jeong¹⁰, Q. Ji¹, Q. P. Ji¹⁹, X. B. Ji^{1,63}, X. L. Ji^{1,58}, Y. Y. Ji⁵⁰, X. Q. Jia⁵⁰, Z. K. Jia^{71,58}, H. J. Jiang⁷⁶, P. C. Jiang^{46,g}, S. S. Jiang³⁹, T. J. Jiang¹⁶, X. S. Jiang^{1,58,63}, Y. Jiang⁶³, J. B. Jiao⁵⁰, Z. Jiao²³, S. Jin⁴², Y. Jin⁶⁶, M. Q. Jing^{1,63}, X. M. Jing⁶³, T. Johansson⁷⁵, X. Kui¹, S. Kabana³³, N. Kalantar-Nayestanaki⁶⁴, X. L. Kang⁹, X. S. Kang⁴⁰, M. Kavatsyuk⁶⁴, B. C. Ke⁸¹, V. Khachatryan²⁷, A. Khoukaz⁶⁸, R. Kiuchi¹, R. Kliemt¹³, O. B. Kolcu^{62A}, B. Kopf³, M. Kuessner³, A. Kupsc^{44,75}, W. Kühn³⁷, J. J. Lane⁶⁷, P. Larin¹⁸, A. Lavania²⁶, L. Lavezzi^{74A,74C}, T. T. Lei^{71,58}, Z. H. Lei^{71,58}, H. Leithoff³⁵, M. Lellmann³⁵, T. Lenz³⁵, C. Li⁴⁷, C. Li⁴³, C. H. Li³⁹, Cheng Li^{71,58}, D. M. Li⁸¹, F. Li^{1,58}, G. Li¹, H. Li^{71,58}, H. B. Li^{1,63}, H. J. Li¹⁹, H. N. Li^{56,i}, Hui Li⁴³, J. R. Li⁶¹, J. S. Li⁵⁹, J. W. Li⁵⁰, Ke Li¹, L. J. Li^{1,63}, L. K. Li¹, Lei Li⁴⁸, M. H. Li⁴³, P. R. Li^{38,k}, Q. X. Li⁵⁰, S. X. Li¹², T. Li⁵⁰, W. D. Li^{1,63}, W. G. Li¹, X. H. Li^{71,58}, X. L. Li⁵⁰, Xiaoyu Li^{1,63}, Y. G. Li^{46,g}, Z. J. Li⁵⁰, Z. X. Li¹⁵, C. Liang⁴², H. Liang^{71,58}, H. Liang^{1,63}, Y. F. Liang⁵⁴, Y. T. Liang^{31,63}, G. R. Liao¹⁴, L. Z. Liao⁵⁰, Y. P. Liao^{1,63}, J. Libby²⁶, A. Limphirat⁶⁰, D. X. Lin^{31,63}, T. Lin¹, B. J. Liu¹, B. X. Liu⁷⁶, C. Liu³⁴, C. X. Liu¹, F. H. Liu⁵³, Fang Liu¹, Feng Liu⁶, G. M. Liu^{56,i}, H. Liu^{38,j,k}, H. B. Liu¹⁵, H. M. Liu^{1,63}, Huanhuan Liu¹, Huihui Liu²¹, J. B. Liu^{71,58}, J. Y. Liu^{1,63}, K. Liu¹, K. Y. Liu⁴⁰, Ke Liu²², L. Liu^{71,58}, L. C. Liu⁴³, Lu Liu⁴³, M. H. Liu^{12,f}, P. L. Liu¹, Q. Liu⁶³, S. B. Liu^{71,58}, T. Liu^{12,f}, W. K. Liu⁴³, W. M. Liu^{71,58}, X. Liu^{38,j,k}, Y. Liu⁸¹, Y. Liu^{38,j,k}, Y. B. Liu⁴³, Z. A. Liu^{1,58,63}, Z. Q. Liu⁵⁰, X. C. Lou^{1,58,63}, F. X. Lu⁵⁹, H. J. Lu²³, J. G. Lu^{1,58}, X. L. Lu¹, Y. Lu⁷, Y. P. Lu^{1,58}, Z. H. Lu^{1,63}, C. L. Luo⁴¹, M. X. Luo⁸⁰, T. Luo^{12,f}, X. L. Luo^{1,58}, X. R. Lyu⁶³, Y. F. Lyu⁴³, F. C. Ma⁴⁰, H. Ma⁷⁹, H. L. Ma¹, J. L. Ma^{1,63}, L. L. Ma⁵⁰, M. M. Ma^{1,63}, Q. M. Ma¹, R. Q. Ma^{1,63}, X. Y. Ma^{1,58}, Y. Ma^{46,g}, Y. M. Ma³¹, F. E. Maas¹⁸, M. Maggiora^{74A,74C}, S. Malde⁶⁹, Q. A. Malik⁷³, A. Mangoni^{28B}, Y. J. Mao^{46,g}, Z. P. Mao¹, S. Marcello^{74A,74C}, Z. X. Meng⁶⁶, J. G. Messchendorp^{13,64}, G. Mezzadri^{29A}, H. Miao^{1,63}, T. J. Min⁴², R. E. Mitchell²⁷, X. H. Mo^{1,58,63}, B. Moses²⁷, N. Yu. Muchnoi^{4,b}, J. Muskalla³⁵, Y. Nefedov³⁶, F. Nerling^{18,d}, I. B. Nikolaev^{4,b}, Z. Ning^{1,58}, S. Nisar^{11,l}, Q. L. Niu^{38,j,k}, W. D. Niu⁵⁵, Y. Niu⁵⁰, S. L. Olsen⁶³, Q. Ouyang^{1,58,63}, S. Pacetti^{28B,28C}, X. Pan⁵⁵, Y. Pan⁵⁷, A. Pathak³⁴, P. Patteri^{28A}, Y. P. Pei^{71,58}, M. Pelizaeus³, H. P. Peng^{71,58}, Y. Y. Peng^{38,j,k}, K. Peters^{13,d}, J. L. Ping⁴¹, R. G. Ping^{1,63}, S. Plura³⁵, V. Prasad³³, F. Z. Qi¹, H. Qi^{71,58}, H. R. Qi⁶¹, M. Qi⁴², T. Y. Qi^{12,f}, S. Qian^{1,58}, W. B. Qian⁶³, C. F. Qiao⁶³, J. J. Qin⁷², L. Q. Qin¹⁴, X. S. Qin⁵⁰, Z. H. Qin^{1,58}, J. F. Qiu¹, S. Q. Qu⁶¹, C. F. Redmer³⁵, K. J. Ren³⁹, A. Rivetti^{74C}, M. Rolo^{74C}, G. Rong^{1,63}, Ch. Rosner¹⁸, S. N. Ruan⁴³, N. Salone⁴⁴, A. Sarantsev^{36,c}, Y. Schelhaas³⁵, K. Schoenning⁷⁵, M. Scodeggio^{29A,29B}, K. Y. Shan^{12,f}, W. Shan²⁴, X. Y. Shan^{71,58}, J. F. Shangguan⁵⁵, L. G. Shao^{1,63}, M. Shao^{71,58}, C. P. Shen^{12,f}, H. F. Shen^{1,63}, W. H. Shen⁶³, X. Y. Shen^{1,63}, B. A. Shi⁶³, H. C. Shi^{71,58}, J. L. Shi¹², J. Y. Shi¹, Q. Q. Shi⁵⁵, R. S. Shi^{1,63}, X. Shi^{1,58}, J. J. Song¹⁹, T. Z. Song⁵⁹, W. M. Song^{34,1}, Y. J. Song¹², Y. X. Song^{46,g}, S. Sosio^{74A,74C}, S. Spataro^{74A,74C}, F. Stieler³⁵, Y. J. Su⁶³, G. B. Sun⁷⁶, G. X. Sun¹, H. Sun⁶³, H. K. Sun¹, J. F. Sun¹⁹, K. Sun⁶¹, L. Sun⁷⁶, S. S. Sun^{1,63}, T. Sun^{51,e}, W. Y. Sun³⁴, Y. Sun⁹, Y. J. Sun^{71,58}, Y. Z. Sun¹, Z. T. Sun⁵⁰, Y. X. Tan^{71,58}, C. J. Tang⁵⁴, G. Y. Tang¹, J. Tang⁵⁹, Y. A. Tang⁷⁶, L. Y. Tao⁷², Q. T. Tao^{25,h}, M. Tat⁶⁹, J. X. Teng^{71,58}, V. Thoren⁷⁵, W. H. Tian⁵², W. H. Tian⁵⁹, Y. Tian^{31,63}, Z. F. Tian⁷⁶, I. Uman^{62B}, Y. Wan⁵⁵, S. J. Wang⁵⁰, B. Wang¹, B. L. Wang⁶³, Bo Wang^{71,58}, C. W. Wang⁴², D. Y. Wang^{46,g}, F. Wang⁷², H. J. Wang^{38,j,k}, J. P. Wang⁵⁰, K. Wang^{1,58}, L. L. Wang¹, M. Wang⁵⁰, Meng Wang^{1,63}, N. Y. Wang⁶³, S. Wang^{12,f}, S. Wang^{38,j,k}, T. Wang^{12,f}, T. J. Wang⁴³, W. Wang⁷², W. Wang⁵⁹, W. P. Wang^{71,58}, X. Wang^{46,g}, X. F. Wang^{38,j,k}, X. J. Wang³⁹, X. L. Wang^{12,f}, Y. Wang⁶¹, Y. D. Wang⁴⁵, Y. F. Wang^{1,58,63}, Y. L. Wang¹⁹, Y. N. Wang⁴⁵, Y. Q. Wang¹, Yaqian Wang^{17,1}, Yi Wang⁶¹, Z. L. Wang^{1,58}, Z. Y. Wang^{1,63}, Ziyi Wang⁶³, D. Wei⁷⁰, D. H. Wei¹⁴, F. Weidner⁶⁸, S. P. Wen¹, C. W. Wenzel³, U. Wiedner³, G. Wilkinson⁶⁹, M. Wolke⁷⁵, L. Wollenberg³, C. Wu³⁹, J. F. Wu^{1,8}, L. H. Wu¹, L. J. Wu^{1,63}, X. Wu^{12,f}, X. H. Wu³⁴, Y. Wu⁷¹, Y. H. Wu⁵⁵, Y. J. Wu³¹, Z. Wu^{1,58}, L. Xia^{71,58}, X. M. Xian³⁹, T. Xiang^{46,g}, D. Xiao^{38,j,k}, G. Y. Xiao⁴², S. Y. Xiao¹, Y. L. Xiao^{12,f}, Z. J. Xiao⁴¹, C. Xie⁴², X. H. Xie^{46,g}, Y. Xie⁵⁰, Y. G. Xie^{1,58}, Y. H. Xie⁶, Z. P. Xie^{71,58}, T. Y. Xing^{1,63}, C. F. Xu^{1,63}, C. J. Xu⁵⁹, G. F. Xu¹, H. Y. Xu⁶⁶, Q. J. Xu¹⁶, Q. N. Xu³⁰, W. X. Xu¹, W. L. Xu⁶⁶, X. P. Xu⁵⁵, Y. C. Xu⁷⁸, Z. P. Xu⁴², Z. S. Xu⁶³, F. Yan^{12,f}, L. Yan^{12,f}, W. B. Yan^{71,58}, W. C. Yan⁸¹, X. Q. Yan¹, H. J. Yang^{51,e}, H. L. Yang³⁴, H. X. Yang¹, Tao Yang¹, Y. Yang^{12,f}, Y. F. Yang⁴³, Y. X. Yang^{1,63}, Yifan Yang^{1,63}, Z. W. Yang^{38,j,k}, Z. P. Yao⁵⁰, M. Ye^{1,58}, M. H. Ye⁸, J. H. Yin¹,

Z. Y. You⁵⁹, B. X. Yu^{1,58,63}, C. X. Yu⁴³, G. Yu^{1,63}, J. S. Yu^{25,h}, T. Yu⁷², X. D. Yu^{46,g}, Y. C. Yu⁸¹, C. Z. Yuan^{1,63}, L. Yuan², S. C. Yuan¹, Y. Yuan^{1,63}, Z. Y. Yuan⁵⁹, C. X. Yue³⁹, A. A. Zafar⁷³, F. R. Zeng⁵⁰, S. H. Zeng⁷², X. Zeng^{12,f}, Y. Zeng^{25,h}, Y. J. Zeng^{1,63}, X. Y. Zhai³⁴, Y. C. Zhai⁵⁰, Y. H. Zhan⁵⁹, A. Q. Zhang^{1,63}, B. L. Zhang^{1,63}, B. X. Zhang¹, D. H. Zhang⁴³, G. Y. Zhang¹⁹, H. Zhang⁷¹, H. C. Zhang^{1,58,63}, H. H. Zhang⁵⁹, H. H. Zhang³⁴, H. Q. Zhang^{1,58,63}, H. Y. Zhang^{1,58}, J. Zhang⁸¹, J. Zhang⁵⁹, J. J. Zhang⁵², J. L. Zhang²⁰, J. Q. Zhang⁴¹, J. W. Zhang^{1,58,63}, J. X. Zhang^{38,j,k}, J. Y. Zhang¹, J. Z. Zhang^{1,63}, Jianyu Zhang⁶³, L. M. Zhang⁶¹, L. Q. Zhang⁵⁹, Lei Zhang⁴², P. Zhang^{1,63}, Q. Y. Zhang^{39,81}, Shuihan Zhang^{1,63}, Shulei Zhang^{25,h}, X. D. Zhang⁴⁵, X. M. Zhang¹, X. Y. Zhang⁵⁰, Y. Zhang⁶⁹, Y. Zhang⁷², Y. T. Zhang⁸¹, Y. H. Zhang^{1,58}, Yan Zhang^{71,58}, Yao Zhang¹, Z. D. Zhang¹, Z. H. Zhang¹, Z. L. Zhang³⁴, Z. Y. Zhang⁴³, Z. Y. Zhang⁷⁶, G. Zhao¹, J. Y. Zhao^{1,63}, J. Z. Zhao^{1,58}, Lei Zhao^{71,58}, Ling Zhao¹, M. G. Zhao⁴³, R. P. Zhao⁶³, S. J. Zhao⁸¹, Y. B. Zhao^{1,58}, Y. X. Zhao^{31,63}, Z. G. Zhao^{71,58}, A. Zhemchugov^{36,a}, B. Zheng⁷², J. P. Zheng^{1,58}, W. J. Zheng^{1,63}, Y. H. Zheng⁶³, B. Zhong⁴¹, X. Zhong⁵⁹, H. Zhou⁵⁰, L. P. Zhou^{1,63}, X. Zhou⁷⁶, X. K. Zhou⁶, X. R. Zhou^{71,58}, X. Y. Zhou³⁹, Y. Z. Zhou^{12,f}, J. Zhu⁴³, K. Zhu¹, K. J. Zhu^{1,58,63}, L. Zhu³⁴, L. X. Zhu⁶³, S. H. Zhu⁷⁰, S. Q. Zhu⁴², T. J. Zhu^{12,f}, W. J. Zhu^{12,f}, Y. C. Zhu^{71,58}, Z. A. Zhu^{1,63}, J. H. Zou¹, J. Zu^{71,58}

(BESIII Collaboration)

¹ Institute of High Energy Physics, Beijing 100049, People's Republic of China

² Beihang University, Beijing 100191, People's Republic of China

³ Bochum Ruhr-University, D-44780 Bochum, Germany

⁴ Budker Institute of Nuclear Physics SB RAS (BINP), Novosibirsk 630090, Russia

⁵ Carnegie Mellon University, Pittsburgh, Pennsylvania 15213, USA

⁶ Central China Normal University, Wuhan 430079, People's Republic of China

⁷ Central South University, Changsha 410083, People's Republic of China

⁸ China Center of Advanced Science and Technology, Beijing 100190, People's Republic of China

⁹ China University of Geosciences, Wuhan 430074, People's Republic of China

¹⁰ Chung-Ang University, Seoul, 06974, Republic of Korea

¹¹ COMSATS University Islamabad, Lahore Campus, Defence Road, Off Raiwind Road, 54000 Lahore, Pakistan

¹² Fudan University, Shanghai 200433, People's Republic of China

¹³ GSI Helmholtzcentre for Heavy Ion Research GmbH, D-64291 Darmstadt, Germany

¹⁴ Guangxi Normal University, Guilin 541004, People's Republic of China

¹⁵ Guangxi University, Nanning 530004, People's Republic of China

¹⁶ Hangzhou Normal University, Hangzhou 310036, People's Republic of China

¹⁷ Hebei University, Baoding 071002, People's Republic of China

¹⁸ Helmholtz Institute Mainz, Staudinger Weg 18, D-55099 Mainz, Germany

¹⁹ Henan Normal University, Xinxiang 453007, People's Republic of China

²⁰ Henan University, Kaifeng 475004, People's Republic of China

²¹ Henan University of Science and Technology, Luoyang 471003, People's Republic of China

²² Henan University of Technology, Zhengzhou 450001, People's Republic of China

²³ Huangshan College, Huangshan 245000, People's Republic of China

²⁴ Hunan Normal University, Changsha 410081, People's Republic of China

²⁵ Hunan University, Changsha 410082, People's Republic of China

²⁶ Indian Institute of Technology Madras, Chennai 600036, India

²⁷ Indiana University, Bloomington, Indiana 47405, USA

²⁸ INFN Laboratori Nazionali di Frascati, (A)INFN Laboratori Nazionali di Frascati, I-00044, Frascati, Italy; (B)INFN Sezione di Perugia, I-06100, Perugia, Italy; (C)University of Perugia, I-06100, Perugia, Italy

²⁹ INFN Sezione di Ferrara, (A)INFN Sezione di Ferrara, I-44122, Ferrara, Italy; (B)University of Ferrara, I-44122, Ferrara, Italy

³⁰ Inner Mongolia University, Hohhot 010021, People's Republic of China

³¹ Institute of Modern Physics, Lanzhou 730000, People's Republic of China

³² Institute of Physics and Technology, Peace Avenue 54B, Ulaanbaatar 13330, Mongolia

³³ Instituto de Alta Investigación, Universidad de Tarapacá, Casilla 7D, Arica 1000000, Chile

³⁴ Jilin University, Changchun 130012, People's Republic of China

³⁵ Johannes Gutenberg University of Mainz, Johann-Joachim-Becher-Weg 45, D-55099 Mainz, Germany

³⁶ Joint Institute for Nuclear Research, 141980 Dubna, Moscow region, Russia

³⁷ Justus-Liebig-Universitaet Giessen, II. Physikalisches Institut, Heinrich-Buff-Ring 16, D-35392 Giessen, Germany

³⁸ Lanzhou University, Lanzhou 730000, People's Republic of China

³⁹ Liaoning Normal University, Dalian 116029, People's Republic of China

⁴⁰ Liaoning University, Shenyang 110036, People's Republic of China

⁴¹ Nanjing Normal University, Nanjing 210023, People's Republic of China

⁴² Nanjing University, Nanjing 210093, People's Republic of China

⁴³ Nankai University, Tianjin 300071, People's Republic of China

⁴⁴ National Centre for Nuclear Research, Warsaw 02-093, Poland

⁴⁵ North China Electric Power University, Beijing 102206, People's Republic of China

⁴⁶ Peking University, Beijing 100871, People's Republic of China

- ⁴⁷ Qufu Normal University, Qufu 273165, People's Republic of China
⁴⁸ Renmin University of China, Beijing 100872, People's Republic of China
⁴⁹ Shandong Normal University, Jinan 250014, People's Republic of China
⁵⁰ Shandong University, Jinan 250100, People's Republic of China
⁵¹ Shanghai Jiao Tong University, Shanghai 200240, People's Republic of China
⁵² Shanxi Normal University, Linfen 041004, People's Republic of China
⁵³ Shanxi University, Taiyuan 030006, People's Republic of China
⁵⁴ Sichuan University, Chengdu 610064, People's Republic of China
⁵⁵ Soochow University, Suzhou 215006, People's Republic of China
⁵⁶ South China Normal University, Guangzhou 510006, People's Republic of China
⁵⁷ Southeast University, Nanjing 211100, People's Republic of China
⁵⁸ State Key Laboratory of Particle Detection and Electronics, Beijing 100049, Hefei 230026, People's Republic of China
⁵⁹ Sun Yat-Sen University, Guangzhou 510275, People's Republic of China
⁶⁰ Suranaree University of Technology, University Avenue 111, Nakhon Ratchasima 30000, Thailand
⁶¹ Tsinghua University, Beijing 100084, People's Republic of China
⁶² Turkish Accelerator Center Particle Factory Group, (A)Istinye University, 34010, Istanbul, Turkey; (B)Near East University, Nicosia, North Cyprus, 99138, Mersin 10, Turkey
⁶³ University of Chinese Academy of Sciences, Beijing 100049, People's Republic of China
⁶⁴ University of Groningen, NL-9747 AA Groningen, The Netherlands
⁶⁵ University of Hawaii, Honolulu, Hawaii 96822, USA
⁶⁶ University of Jinan, Jinan 250022, People's Republic of China
⁶⁷ University of Manchester, Oxford Road, Manchester, M13 9PL, United Kingdom
⁶⁸ University of Muenster, Wilhelm-Klemm-Strasse 9, 48149 Muenster, Germany
⁶⁹ University of Oxford, Keble Road, Oxford OX13RH, United Kingdom
⁷⁰ University of Science and Technology Liaoning, Anshan 114051, People's Republic of China
⁷¹ University of Science and Technology of China, Hefei 230026, People's Republic of China
⁷² University of South China, Hengyang 421001, People's Republic of China
⁷³ University of the Punjab, Lahore-54590, Pakistan
⁷⁴ University of Turin and INFN, (A)University of Turin, I-10125, Turin, Italy; (B)University of Eastern Piedmont, I-15121, Alessandria, Italy; (C)INFN, I-10125, Turin, Italy
⁷⁵ Uppsala University, Box 516, SE-75120 Uppsala, Sweden
⁷⁶ Wuhan University, Wuhan 430072, People's Republic of China
⁷⁷ Xinyang Normal University, Xinyang 464000, People's Republic of China
⁷⁸ Yantai University, Yantai 264005, People's Republic of China
⁷⁹ Yunnan University, Kunming 650500, People's Republic of China
⁸⁰ Zhejiang University, Hangzhou 310027, People's Republic of China
⁸¹ Zhengzhou University, Zhengzhou 450001, People's Republic of China
- ^a Also at the Moscow Institute of Physics and Technology, Moscow 141700, Russia
^b Also at the Novosibirsk State University, Novosibirsk, 630090, Russia
^c Also at the NRC "Kurchatov Institute", PNPI, 188300, Gatchina, Russia
^d Also at Goethe University Frankfurt, 60323 Frankfurt am Main, Germany
^e Also at Key Laboratory for Particle Physics, Astrophysics and Cosmology, Ministry of Education; Shanghai Key Laboratory for Particle Physics and Cosmology; Institute of Nuclear and Particle Physics, Shanghai 200240, People's Republic of China
^f Also at Key Laboratory of Nuclear Physics and Ion-beam Application (MOE) and Institute of Modern Physics, Fudan University, Shanghai 200443, People's Republic of China
^g Also at State Key Laboratory of Nuclear Physics and Technology, Peking University, Beijing 100871, People's Republic of China
^h Also at School of Physics and Electronics, Hunan University, Changsha 410082, China
ⁱ Also at Guangdong Provincial Key Laboratory of Nuclear Science, Institute of Quantum Matter, South China Normal University, Guangzhou 510006, China
^j Also at MOE Frontiers Science Center for Rare Isotopes, Lanzhou University, Lanzhou 730000, People's Republic of China
^k Also at Lanzhou Center for Theoretical Physics, Lanzhou University, Lanzhou 730000, People's Republic of China
^l Also at the Department of Mathematical Sciences, IBA, Karachi 75270, Pakistan

(Dated: April 1, 2024)

We perform for the first time an amplitude analysis of the decay $D^+ \rightarrow K_S^0 \pi^+ \eta$ and report the observation of the decay $D^+ \rightarrow K_S^0 a_0(980)^+$ using 2.93 fb^{-1} of $e^+ e^-$ collision data taken at a center-of-mass energy of 3.773 GeV with the BESIII detector. As the only W -annihilation-free decay among D to $a_0(980)$ -pseudoscalar $D^+ \rightarrow K_S^0 a_0(980)^+$ is the ideal decay in extracting the contributions of the W -emission amplitudes involving $a_0(980)$ and to study the final-state interactions. The absolute branching fraction of $D^+ \rightarrow K_S^0 \pi^+ \eta$ is measured to be $(1.27 \pm 0.04_{\text{stat.}} \pm 0.03_{\text{syst.}})\%$. The branching fractions of intermediate processes $D^+ \rightarrow K_S^0 a_0(980)^+$ with $a_0(980)^+ \rightarrow \pi^+ \eta$ and

$D^+ \rightarrow \pi^+ \bar{K}_0^*(1430)^0$ with $\bar{K}_0^*(1430)^0 \rightarrow K_S^0 \eta$ are measured to be $(1.33 \pm 0.05_{\text{stat.}} \pm 0.04_{\text{syst.}})\%$ and $(0.14 \pm 0.03_{\text{stat.}} \pm 0.01_{\text{syst.}})\%$, respectively.

Perturbative quantum chromodynamics (QCD) approaches, such as QCD factorization and soft-collinear effective theory, have well explained physics of nonleptonic b -hadron decays [1–4]. However, the charm quark mass is located between the perturbative and nonperturbative QCD regions, making neither of those approaches applicable. As a result, an accurate theoretical description of the underlying mechanism for exclusive hadronic decays of charmed mesons is still not available. A model-independent analysis was then proposed in the so-called diagrammatic approach to phenomenologically describe charmed meson decays [5]. The diagrammatic approach represents the W -emission and weak-annihilation (W -exchange or W -annihilation) amplitudes as topological quark-graph diagrams based on SU(3) flavor symmetry. With necessary experimental inputs, it enables us to extract the contribution and study the relative importance of each amplitude.

On the other hand, great progress has been achieved by a series of amplitude analyses on the hadronic charmed meson decays [6–16]. According to these studies, D meson decays are dominated by quasi-two-body processes, such as $D \rightarrow PP$, VP , SP , AP , and TP , where P , V , S , A , and T denote pseudoscalar, vector, scalar, axial-vector, and tensor mesons, respectively. These enriching experimental results allow the diagrammatic approach to be applied quite successfully in $D \rightarrow PP$ and $D \rightarrow VP$ decays [17, 18]. However, in the sector of $D \rightarrow SP$, it appears that the current experimental measurements are still insufficient [19–30], and the decay $D^+ \rightarrow K_S^0 a_0(980)^+$ is the most urgently needed and ideal decay to test the validity of the diagrammatic approach.

A large discrepancy between experimental results and theoretical predictions of branching fractions (BFs) for many $D^{+,0} \rightarrow a_0(980)P$ decays have been found [19–21]. The main reason could be ascribed to the contribution of the weak-annihilation amplitudes in D decays, which are hard to estimate accurately. Among $D^{+,0} \rightarrow a_0(980)P$, $D^+ \rightarrow K_S^0 a_0(980)^+$ is the only decay free of weak-annihilation contributions, as depicted in Fig. 1, and mainly involves the internal W -emission in Fig. 2(a), while its BF is not theoretically predicted. Without the interference from weak annihilation, the study of $D^+ \rightarrow K_S^0 a_0(980)^+$ will serve as a key experimental input and provide the most sensitive constraint to the contributions and phases of the internal W -emission amplitudes involving $a_0(980)$ in the diagrammatic approach method [19–21]. It is worth noting that the external W -emission amplitude for this decay is naively expected to be rather suppressed compared to the internal one, due to G -parity violation [31, 32]. In addition, the light scalar particle $a_0(980)$ is commonly con-

sidered as a candidate for exotic states, which are states other than typical quark-antiquark mesons, such as states for tetraquarks, $K\bar{K}$ bound states, and other possible states. The production of these exotic states essentially involves final-state interactions, such as quark exchange, resonance formation, etc. [31–36]. For example, the production of the tetraquark $a_0(980)^+$ state in D^+ decays can occur as a result of the fact that the seed tetraquark fluctuations $u\bar{d} \rightarrow \pi^+\eta$, $\pi^+\eta'$, $K^+\bar{K}^0$ are dressed by strong resonance interactions in the final state [36]. Figure 2(d) also illustrates an example of the production of the tetraquark $a_0(980)^+$ state due to rescattering in the final state. Studying $D^+ \rightarrow K_S^0 a_0(980)^+$ can experimentally constrain the contribution from these effects, which helps to pin down the nature of $a_0(980)$.

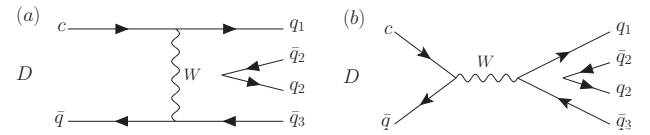


FIG. 1. (a) The W -exchange and (b) the W -annihilation diagrams for D decays. For the D^+ meson, the W -exchange mechanism is simply absent. The W -annihilation mechanism cannot generate the hadronic mode with a \bar{K}^0 in the final state.

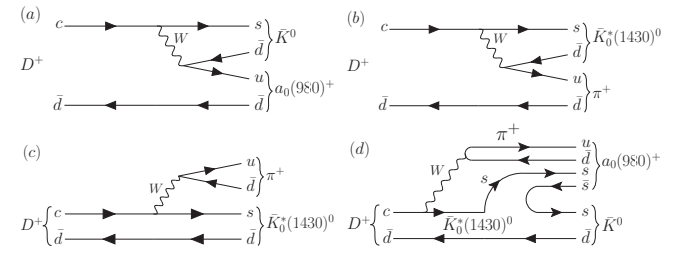


FIG. 2. (a) The internal W -emission diagram for the decay $D^+ \rightarrow \bar{K}_0^* a_0(980)^+$ by assuming $a_0(980)^+$ is a two-quark state. (b) The internal and (c) the external W -emission diagrams for the decay $D^+ \rightarrow \bar{K}_0^*(1430)^0 \pi^+$. (d) An example diagram of $D^+ \rightarrow \bar{K}_0^* a_0(980)^+$ via rescattering in the final state of $D^+ \rightarrow \bar{K}_0^*(1430)^0 \pi^+$ under the assumption that $a_0(980)^+$ is a tetraquark state.

Moreover, precision measurements of absolute hadronic D meson BFs are essential for both charm and beauty physics. The $D^+ \rightarrow K_S^0 \pi^+ \eta$ decay, dominated by the Cabibbo-favored process, has a large BF of the order of 10^{-2} . This decay contains other possible intermediate amplitudes, such as $\bar{K}_0^*(1430)^0 \pi^+$, as depicted in Figs. 2(b) and 2(c). Studying the relative contribution of the intermediate resonances can not only benefit the understanding of the strong interaction at low energies but also determine these missing D^+ decay

modes.

The BESIII detector collected 2.93 fb^{-1} of e^+e^- collision data in 2010 and 2011 at $\sqrt{s} = 3.773 \text{ GeV}$ [37], which corresponds to the mass of the $\psi(3770)$ resonance. The $\psi(3770)$ decays predominantly to $D^0\bar{D}^0$ or $D^+\bar{D}^-$ without any additional hadrons. The excellent tracking, precision calorimetry, and the large $D\bar{D}$ threshold data sample provide an unprecedented opportunity to study the charmed meson decays. Based on this dataset, we present the first amplitude analysis of the decay $D^+ \rightarrow K_S^0\pi^+\eta$ [38] and report the observation of the decay $D^+ \rightarrow K_S^0a_0(980)$. Charge-conjugate states are implied throughout this Letter.

The BESIII detector [39] records the final-state particles of symmetric e^+e^- collisions provided by the BEPCII storage ring [40] in the center-of-mass energy range from 2.00 to 4.95 GeV, with a peak luminosity of $1 \times 10^{33} \text{ cm}^{-2}\text{s}^{-1}$ achieved at $\sqrt{s} = 3.77 \text{ GeV}$. The cylindrical core of the BESIII detector covers 93% of the full solid angle and consists of a helium-based multilayer drift chamber, a plastic scintillator time-of-flight system, and a CsI(Tl) electromagnetic calorimeter, which are all enclosed in a superconducting solenoidal magnet providing a 1.0 T magnetic field.

Simulated data samples produced with a GEANT4-based [41] Monte Carlo (MC) toolkit, which includes the geometric description [42] of the BESIII detector and the detector response, are used to determine detection efficiencies and to estimate backgrounds. The simulation models the beam energy spread and initial state radiation (ISR) in the e^+e^- annihilations with the generator KKMC [43]. The inclusive MC sample includes the production of $D\bar{D}$ pairs (including quantum coherence for the neutral D channels), the non- $D\bar{D}$ decays of the $\psi(3770)$, the ISR production of the J/ψ and $\psi(3686)$ states, and the continuum processes incorporated in KKMC. All particle decays are modelled with EVTGEN [44] using BFs either taken from the Particle Data Group (PDG) [6], when available, or otherwise estimated with LUNDCHARM [45]. Final-state radiation from charged final-state particles is incorporated using PHOTOS [46].

By fully reconstructing the D^+D^- meson pairs, a double-tag (DT) method provides samples with high purity to perform amplitude analyses and measurements of absolute BFs of the hadronic D^+ meson decays. The DT candidates are required to be the D^+ meson decaying to the signal mode $D^+ \rightarrow K_S^0\pi^+\eta$ and the D^- meson decaying to six tag modes: $K^+\pi^-\pi^-$, $K_S^0\pi^-$, $K^+\pi^-\pi^-\pi^0$, $K_S^0\pi^-\pi^0$, $K_S^0\pi^-\pi^-\pi^+$, or $K^+K^-\pi^-$. The selection criteria for the final-state particles are the same as in Ref. [38].

The D^\pm mesons are selected using two variables, the energy difference $\Delta E = E_D - E_b$ and the beam-constrained mass $M_{BC} = \sqrt{E_b^2 - |\vec{p}_D|^2}$, where E_b is the

beam energy and \vec{p}_D and E_D are the momentum and the energy of the D^\pm candidate in the e^+e^- rest frame, respectively. The D^- meson is reconstructed first through the six tag modes. In case of multiple candidates, the one with the minimum $|\Delta E|$ is chosen. Once a tag is identified, the signal decay $D^+ \rightarrow K_S^0\pi^+\eta$ is searched for at the recoiling side and the best signal candidate with the minimum $|\Delta E|$ is selected. All D^\pm candidates are required to satisfy $1.865 < M_{BC} < 1.875 \text{ GeV}$, and $-0.055 < \Delta E < 0.040 \text{ GeV}$ for the tag modes containing π^0 in the final state, $-0.025 < \Delta E < 0.025 \text{ GeV}$ for the others, and $-0.020 < \Delta E < 0.020 \text{ GeV}$ for the signal side. In addition, the energy of the largest unused photons is required to be less than 0.23 GeV. There are 1113 DT events obtained for the amplitude analysis with a signal purity of $(98.2 \pm 0.4)\%$, which is determined from a two-dimensional unbinned maximum-likelihood fit to the distribution of M_{BC} of the tag D^- versus that of the signal D^+ . (Details of the fit are introduced in Ref. [38].)

The amplitude analysis requires a sample with good resolution and all candidates falling within the phase-space boundary. Therefore, a four-constraint kinematic fit is performed, assuming D^- candidates decaying to one of the tag modes and D^+ decaying to the signal mode. The invariant masses of $(\gamma\gamma)_\eta$, $(\pi^+\pi^-)_{K_S^0}$, and D^\pm candidates are constrained to their individual known masses [6]. The Dalitz plot of the $D^+ \rightarrow K_S^0\pi^+\eta$ candidates for the data sample is shown in Fig. 3(a).

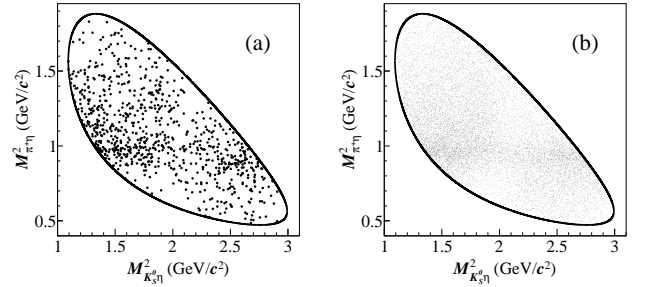


FIG. 3. The Dalitz plots of $M_{\pi^+\eta}^2$ versus $M_{K_S^0\eta}^2$ of the $D^+ \rightarrow K_S^0\pi^+\eta$ candidates for (a) the data sample and (b) the signal MC sample generated according to the amplitude analysis results.

The intermediate-resonance composition is determined by an unbinned maximum-likelihood fit. The likelihood function \mathcal{L} is constructed with a signal probability density function (PDF), which depends on the momenta p of the three final-state particles: $\mathcal{L} = \prod_j^{N_D} f(p_j^k)$, where j runs over the three final-state particles, k runs over each data event, N_D is the number of candidate events in data, and f is the signal PDF. To take the background into account, its contribution is subtracted from the data by

modifying the negative-likelihood function as follows [47]:

$$-\ln \mathcal{L} = \frac{-N_D + w N_B}{N_D + w^2 N_B} \left[\sum_k^{N_D} \ln f(p_j^k) - \sum_l^{N_B} w \ln f(p_j^l) \right], \quad (1)$$

where l runs over each background event obtained from the inclusive MC sample, N_B is the number of these background events, and the weight $w = (1 - \text{purity})N_D/N_B$ is normalized to data based on the signal purity.

The signal PDF is written as

$$f_S(p_j) = \frac{\epsilon(p_j) |\mathcal{M}(p_j)|^2 R_3}{\int \epsilon(p_j) |\mathcal{M}(p_j)|^2 R_3 dp_j}, \quad (2)$$

where $\epsilon(p_j)$ is the detection efficiency and R_3 is the standard element of three-body phase space (see Sec. 49, “Kinematics,” in Ref. [6]). The total amplitude, $\mathcal{M}(p_j)$, is the coherent sum of individual amplitudes of intermediate processes, $\sum \rho_n e^{i\phi_n} \mathcal{A}_n$, where ρ_n and ϕ_n are the magnitude and phase for the amplitude \mathcal{A}_n of the n th intermediate resonance, respectively. The amplitude \mathcal{A}_n is the product of the spin factor [48], the Blatt-Weisskopf barriers of the intermediate state and the D^+ meson [49], and the propagator for the intermediate resonance. The propagator of $a_0(980)^+$ is parametrized with a Flatté formula and the parameters are fixed to the values given in Ref. [50]. The propagator of $\bar{K}_0^*(1430)^0$ is parametrized as a relativistic Breit-Wigner (RBW) function [51] using parameters obtained in Ref. [52]. The normalization integral term in the denominator is handled by MC integration [12].

In the fit, the magnitude and phase of the amplitude $D^+ \rightarrow K_S^0 a_0(980)^+$ are fixed to 1.0 and 0.0, respectively, while those of other amplitudes are left floating. Various combinations of amplitudes for intermediate resonances are tested. The statistical significance of each amplitude is calculated based on the change of the log-likelihood with and without this amplitude after taking the change of the degrees of freedom into account. Two dominant amplitudes with significance greater than 5σ , $D^+ \rightarrow K_S^0 a_0(980)^+$ and $D^+ \rightarrow \bar{K}_0^*(1430)^0 \pi^+$, remain as the nominal set. Other amplitudes for possible intermediate resonances, including $D^+ \rightarrow \bar{K}_1(1270)^0 \pi^+$, $D^+ \rightarrow K^*(1410)^+ \eta$, $D^+ \rightarrow K_2^*(1430)^+ \eta$, $D^+ \rightarrow \bar{K}_2^*(1580)^0 \pi^+$, $D^+ \rightarrow K_S^0 \pi_1(1400)^+$, $D^+ \rightarrow K_S^0 a_0(1450)^+$, $D^+ \rightarrow K_S^0 a_2(1320)^+$, $D^+ \rightarrow K^*(892)^+ \eta$, and $D^+ \rightarrow (K_S^0 \pi^+)_S \text{-wave} \eta$ (using the LASS parametrization [53]), have no significant contribution. The contribution of the n th intermediate process relative to the total BF is quantified by a fit fraction (FF) defined as

$$\text{FF}_n = \frac{\sum_{\text{gen}}^{N_{\text{gen}}} |\rho_n e^{i\phi_n} \mathcal{A}_n|^2}{\sum_{\text{gen}}^{N_{\text{gen}}} |\mathcal{M}|^2}, \quad (3)$$

where N_{gen} is the number of the generated phase-space MC events. The statistical uncertainties of FFs are determined by sampling randomly according to the Gaussian

distributions of $\text{FF}_{a_0(980)^+}$ and $\text{FF}_{\bar{K}_0^*(1430)^0}$ and to their correlation through the covariance matrix.

The phases, FFs, and statistical significances for the amplitudes are listed in Table I. The Dalitz plot for the signal MC sample generated based on the amplitude analysis model is shown in Fig. 3(b). The Dalitz plot projections are shown in Fig. 4. The correlation matrix is provided in Table II. The systematic uncertainties of the amplitude analysis, as summarized in Table III, are estimated as described below.

The systematic uncertainty due to the $a_0(980)^+$ line shape is estimated by varying the mass and coupling constant of the Flatté propagator by $\pm 1\sigma$ and a three-channel-coupled Flatté formula which adds the $\pi\eta'$ according to Ref. [50]. The systematic uncertainty caused by the $\bar{K}_0^*(1430)^0$ line shape is estimated by varying the mass and width of the RBW by $\pm 1\sigma$ according to Ref. [52]. The quadratic sum of these two uncertainties is taken to be the amplitude model systematic uncertainty. The systematic uncertainty due to the effective radius of the Blatt-Weisskopf barrier [49] is determined by varying the effective radius within the range [2.0, 4.0] GeV for intermediate resonances and [4.0, 6.0] GeV for D^+ mesons. The maximum variations are taken as the systematic uncertainties. The uncertainties caused by possible but insignificant intermediate resonances, such as $\bar{K}_1(1270)^0 \pi^+$, $K^*(1410)^+ \eta$, $\bar{K}_2^*(1580)^0 \pi^+$, $K_S^0 a_0(1450)^+$, and $K_S^0 a_2(1320)^+$, are taken to be the differences of the phases and FFs with and without the intermediate resonances.

To determine the systematic uncertainty related to the background estimation, the sPlot technique [54] is instead employed on the M_{BC} variable to eliminate the combinatorial background. An amplitude analysis, after applying sWeights, is performed, and deviations from the nominal results are assigned as the systematic uncertainties. The uncertainty associated with the detector acceptance difference between MC samples and data is determined by reweighting $\epsilon(p_j)$ in Eq. 2 with different reconstruction efficiencies of K_S^0 , π^+ , and η according to their uncertainties. The changes of the fit results are taken as the systematic uncertainties. In addition, with the amplitude analysis results obtained in this work, 300 signal MC samples are generated with the same size as data. The pull value is calculated by $V_{\text{pull}} = (V_{\text{fit}} - V_{\text{input}})/\sigma_{\text{fit}}$, where V_{input} is the input value in the generator and V_{fit} and σ_{fit} are the output value and corresponding statistical uncertainty, respectively. The resulting pull distributions are consistent with the standardized normal distributions, showing no significant fit bias.

The BF of $D^+ \rightarrow K_S^0 \pi^+ \eta$ was previously measured in Ref. [38]. We update this BF to be $(1.27 \pm 0.04_{\text{stat.}} \pm 0.03_{\text{syst.}})\%$ with a signal MC sample generated based on the amplitude analysis model, which provides a more

TABLE I. Phases, FFs, and statistical significances for different amplitudes. The first uncertainty is statistical, while the second and third uncertainties are model and experimental systematic uncertainties, respectively. The total of the FFs is not necessarily equal to 100% due to interference effects.

Amplitude	Phase ϕ (rad)	FF (%)	Significance
$D^+ \rightarrow K_S^0 a_0(980)^+$	0.0(fixed)	$105.00 \pm 0.94 \pm 1.04 \pm 0.07$	$> 10\sigma$
$D^+ \rightarrow \bar{K}_0^*(1430)^0 \pi^+$	$2.58 \pm 0.06 \pm 0.09 \pm 0.01$	$10.83 \pm 1.50 \pm 1.27 \pm 0.08$	$> 10\sigma$

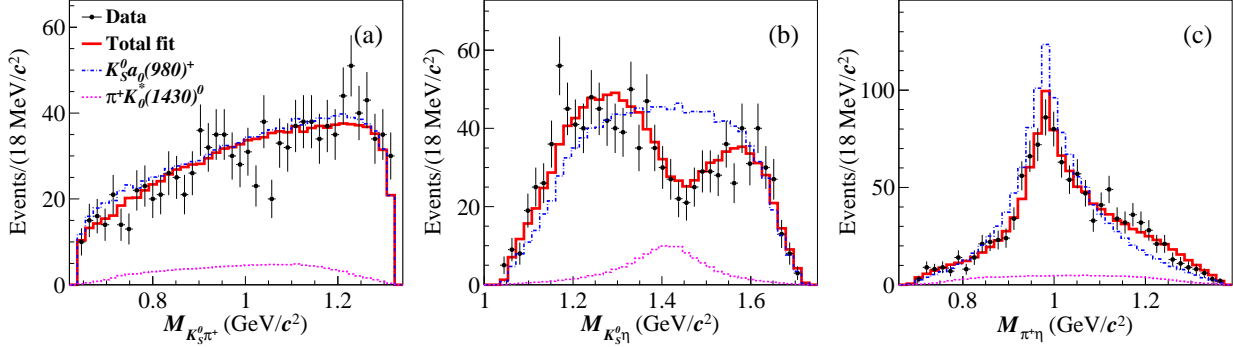


FIG. 4. Projections on the invariant masses of (a) $K_S^0 \pi^+$, (b) $K_S^0 \eta$, and (c) $\pi^+ \eta$ systems of the nominal fit. The data are represented by black dots with the error bars, the fit results by the solid red curves with the $K_S^0 a_0(980)^+$ yields by the dashed blue curves and the $\bar{K}_0^*(1430)^0 \pi^+$ yields by the dashed magenta curves. The fit results take into account the relative phases and interferences between the two signal amplitudes, making a simple visual addition of the lines of the two signal amplitudes insufficient. The impact of the destructive interference is clearly visible in (b). Background is not shown as it is almost negligible graphically.

TABLE II. Correlation matrix for the phases and FFs.

	FF $a_0(980)^+$	FF $\bar{K}_0^*(1430)^0$	$\phi_{\bar{K}_0^*(1430)^0}$
FF $a_0(980)^+$	1.00	-0.28	0.88
FF $\bar{K}_0^*(1430)^0$		1.00	0.20
$\phi_{\bar{K}_0^*(1430)^0}$			1.00

TABLE III. Systematic uncertainties on the phases and FFs for different amplitudes in units of statistical uncertainties. The sources are categorized as: Model - (I) Amplitude model, (II) Effect radius, and (III) Insignificant resonances; Experimental (Exp.) - (IV) Background and (V) Detector acceptance.

Amplitude	Model					Exp. Total
	I	II	III	IV	V	
$D^+ \rightarrow K_S^0 a_0(980)^+$	FF 0.32	0.01	1.06	0.10	0.04	1.11
$D^+ \rightarrow \pi^+ \bar{K}_0^*(1430)^0$	ϕ 0.47	0.01	1.33	0.13	0.08	1.42
	FF 0.12	0.01	0.84	0.04	0.05	0.85

precise estimation of the detection efficiency. The uncertainty associated with the amplitude analysis model, 0.7%, is estimated by varying the model parameters based on their error matrix.

In summary, we perform an amplitude analysis of

$D^+ \rightarrow K_S^0 \pi^+ \eta$ for the first time and report the observation of $D^+ \rightarrow K_S^0 a_0(980)^+$. The interferences between intermediate resonances are fully considered and a $(15.83 \pm 1.53_{\text{stat.}} \pm 1.65_{\text{syst.}})\%$ destructive interference is observed between the $D^+ \rightarrow K_S^0 a_0(980)^+$ and $D^+ \rightarrow \bar{K}_0^*(1430)^0 \pi^+$ amplitudes. The amplitude analysis results are listed in Table I. With a detection efficiency obtained with MC samples according to the amplitude analysis model, we obtain $\mathcal{B}(D^+ \rightarrow K_S^0 \pi^+ \eta) = (1.27 \pm 0.04_{\text{stat.}} \pm 0.03_{\text{syst.}})\%$. This work uses the same datasets as the previous measurement of $(1.31 \pm 0.05)\%$ did [6, 38], whereas the small difference arises from the change of the signal model from a modified data-driven generator BODY3 [55] to the amplitude analysis model, which is used to estimate the detection efficiency.

Using the FFs listed in Table I, the BFs for the intermediate processes are calculated as $\mathcal{B}_i = \text{FF}_i \times \mathcal{B}(D^+ \rightarrow K_S^0 \pi^+ \eta)$ to be $\mathcal{B}(D^+ \rightarrow K_S^0 a_0(980)^+, a_0(980)^+ \rightarrow \pi^+ \eta) = (1.33 \pm 0.05_{\text{stat.}} \pm 0.04_{\text{syst.}})\%$ and $\mathcal{B}(D^+ \rightarrow \bar{K}_0^*(1430)^0 \pi^+, \bar{K}_0^*(1430)^0 \rightarrow K_S^0 \eta) = (0.14 \pm 0.02_{\text{stat.}} \pm 0.02_{\text{syst.}})\%$. Theoretical studies insistently require experimental measurements of $D^+ \rightarrow K_S^0 a_0(980)^+$, as its observation can provide sensitive constraints in the extraction of contributions from internal W -emission diagrams of $D \rightarrow SP$ [19–21]. If these measured BFs cannot be well described by the diagrammatic approach it would indicate that significant final-state interactions

must be involved [36], which will provide critical information on the role of $a_0(980)$ in charmed meson decays and the nature of $a_0(980)$. In addition, the BF of $D^+ \rightarrow \bar{K}_0^*(1430)^0 \pi^+$ obtained in this work, $(3.26 \pm 0.47_{\text{stat.}} \pm 0.47_{\text{syst.}} {}^{+1.02}_{-1.29} K_0^*)\%$ ¹, is consistent with that derived from $D^+ \rightarrow K^- \pi^+ \pi^+$ and $D^+ \rightarrow K_S^0 \pi^+ \pi^0$ by the PDG, $(2.02 \pm 0.10_{\text{stat.}} \pm 0.22_{\text{syst.}})\%$ [6]. In the near future, we plan to use 20 fb^{-1} data to conduct a more precise investigation into the production of $a_0(980)$ and $f_0(980)$ in D -meson decays [56–58].

The BESIII Collaboration thanks the staff of BEPCII and the IHEP computing center for their strong support. The authors thank Prof. Yu-Kuo Hsiao for helpful discussions. This work is supported in part by National Key R&D Program of China under Contracts Nos. 2020YFA0406400, 2020YFA0406300; National Natural Science Foundation of China (NSFC) under Contracts Nos. 11635010, 11735014, 11835012, 11875054, 11935015, 11935016, 11935018, 11961141012, 12022510, 12025502, 12035009, 12035013, 12061131003, 12192260, 12192261, 12192262, 12192263, 12192264, 12192265, 12221005, 12225509, 12235017, 12205384; the Chinese Academy of Sciences (CAS) Large-Scale Scientific Facility Program; the CAS Center for Excellence in Particle Physics (CCEPP); Joint Large-Scale Scientific Facility Funds of the NSFC and CAS under Contract Nos. U2032104, U1832207; CAS Key Research Program of Frontier Sciences under Contracts Nos. QYZDJ-SSW-SLH003, QYZDJ-SSW-SLH040; 100 Talents Program of CAS; The Institute of Nuclear and Particle Physics (INPAC) and Shanghai Key Laboratory for Particle Physics and Cosmology; ERC under Contract No. 758462; European Union’s Horizon 2020 research and innovation programme under Marie Skłodowska-Curie grant agreement under Contract No. 894790; German Research Foundation DFG under Contracts Nos. 443159800, 455635585, Collaborative Research Center CRC 1044, FOR5327, GRK 2149; Istituto Nazionale di Fisica Nucleare, Italy; Ministry of Development of Turkey under Contract No. DPT2006K-120470; National Research Foundation of Korea under Contract No. NRF-2022R1A2C1092335; National Science and Technology fund of Mongolia; National Science Research and Innovation Fund (NSRF) via the Program Management Unit for Human Resources & Institutional Development, Research and Innovation of Thailand under Contract No. B16F640076; Polish National Science Centre under Contract No. 2019/35/O/ST2/02907; The Swedish Research Council; U. S. Department of Energy under Contract No. DE-FG02-05ER41374

¹ The third uncertainty comes from the BF of $\bar{K}_0^*(1430)^0 \rightarrow K^0 \eta$, $(8.6 {}^{+2.7}_{-3.4})\%$ [6].

-
- [1] M. Beneke, G. Buchalla, M. Neubert and C. T. Sachrajda, *Nucl. Phys. B* **606**, 245 (2001).
 - [2] A. K. Leibovich, Z. Ligeti, I. W. Stewart and M. B. Wise, *Phys. Lett. B* **586**, 337 (2004).
 - [3] J. J. Han, Y. Li, H. n. Li, Y. L. Shen, Z. J. Xiao and F. S. Yu, *Eur. Phys. J. C* **82**, 686 (2022).
 - [4] Y. K. Hsiao, *Phys. Lett. B* **845**, 138158 (2023).
 - [5] L. L. Chau and H. Y. Cheng, *Phys. Rev. Lett.* **56**, 1655 (1986).
 - [6] R. L. Workman *et al.* (Particle Data Group), *Prog. Theor. Exp. Phys.* **2022**, 083C01 (2022).
 - [7] M. Ablikim *et al.* (BESIII Collaboration), *J. High Energy Phys.* **09** (2022) 242.
 - [8] M. Ablikim *et al.* (BESIII Collaboration), *J. High Energy Phys.* **08** (2022) 196.
 - [9] M. Ablikim *et al.* (BESIII Collaboration), *J. High Energy Phys.* **07** (2022) 051.
 - [10] M. Ablikim *et al.* (BESIII Collaboration), *J. High Energy Phys.* **04** (2022) 058.
 - [11] M. Ablikim *et al.* (BESIII Collaboration), *J. High Energy Phys.* **01** (2022) 052.
 - [12] M. Ablikim *et al.* (BESIII Collaboration), *Phys. Rev. Lett.* **129**, 182001 (2022).
 - [13] M. Ablikim *et al.* (BESIII Collaboration), *Phys. Rev. D* **103**, 092006 (2021).
 - [14] M. Ablikim *et al.* (BESIII Collaboration), *Phys. Rev. D* **99**, 092008 (2019).
 - [15] M. Ablikim *et al.* (BESIII Collaboration), *Phys. Rev. Lett.* **123**, 112001 (2019).
 - [16] M. Ablikim *et al.* (BESIII Collaboration), *Phys. Rev. D* **95**, 072010 (2017).
 - [17] H. Y. Cheng and C. W. Chiang, *Phys. Rev. D* **100**, 093002 (2019).
 - [18] H. Y. Cheng and C. W. Chiang, *Phys. Rev. D* **81**, 074021 (2010).
 - [19] H. Y. Cheng, C. W. Chiang, and Z. Q. Zhang, *Phys. Rev. D* **105**, 033006 (2022).
 - [20] H. Y. Cheng, *Phys. Rev. D* **67**, 034024 (2003).
 - [21] H. Y. Cheng and C. W. Chiang, *Phys. Rev. D* **81**, 074031 (2010).
 - [22] F. Hussain, A. N. Kamal, and S. N. Sinha, *Z. Phys. C* **36**, 199 (1987).
 - [23] A. C. Katoch and R. C. Verma, *Z. Phys. C* **62**, 173 (1994).
 - [24] S. Fajfer, *Z. Phys. C* **68**, 81 (1995).
 - [25] F. Buccella, F. and M. Lusignoli, and A. Pugliese, *Phys. Lett. B* **379**, 249 (1996).
 - [26] B. El-Bennich, O. Leitner, J. P. Dedonder, and B. Loiseau, *Phys. Rev. D* **79**, 076004 (2009).
 - [27] D. R. Boito, J. P. Dedonder, B. El-Bennich, O. Leitner, and B. Loiseau, *Phys. Rev. D* **79**, 034020 (2009).
 - [28] J. P. Dedonder, R. Kamiński, L. Lesniak, B. Loiseau, *Phys. Rev. D* **89**, 094018 (2014).
 - [29] J. J. Xie, L. R. Dai, and E. Oset, *Phys. Lett. B* **742**, 363 (2015).
 - [30] J. P. Dedonder, R. Kamiński, L. Lesniak, B. Loiseau, *Phys. Rev. D* **103**, 114028 (2021).
 - [31] Y. K. Hsiao, Y. Yu, and B. C. Ke, *Eur. Phys. J. C* **80**, 895 (2020).
 - [32] Y. Yu, Y. K. Hsiao, and B. C. Ke, *Eur. Phys. J. C* **81**, 1093 (2021).

- [33] Y. K. Hsiao, S. Q. Yang, W. J. Wei, and B. C. Ke, arXiv:2306.06091 [hep-ph].
- [34] H. Zhang, Y. H. Lyu, L. J. Liu, E. Wang, Chin. Phys. C **47**, 043101 (2023).
- [35] N. N. Achasov and G. N. Shestakov, Phys. Rev. D **96**, no.3, 036013 (2017).
- [36] N. N. Achasov, A. V. Kiselev and G. N. Shestakov, Phys. Rev. D **104**, no.1, 016034 (2021).
- [37] M. Ablikim *et al.* (BESIII Collaboration), Chin. Phys. C **37**, 123001 (2013).
- [38] M. Ablikim *et al.* (BESIII Collaboration), Phys. Rev. Lett. **124**, 241803 (2020).
- [39] M. Ablikim *et al.* (BESIII Collaboration), Nucl. Instrum. Methods Phys. Res. Sect. A **614**, 345 (2010).
- [40] C. H. Yu *et al.*, Proceedings of IPAC2016, Busan, Korea, 2016, doi:10.18429/JACoW-IPAC2016-TUYA01.
- [41] S. Agostinelli *et al.* (GEANT4 Collaboration), Nucl. Instrum. Meth. A **506**, 250 (2003).
- [42] K. X. Huang, *et al.*, Nucl. Sci. Tech. **33**, 142 (2022).
- [43] S. Jadach, B. F. L. Ward, and Z. Was, Phys. Rev. D **63**, 113009 (2001); Comput. Phys. Commun. **130**, 260 (2000).
- [44] D. J. Lange, Nucl. Instrum. Meth. A **462**, 152 (2001); R. G. Ping, Chin. Phys. C **32**, 599 (2008).
- [45] J. C. Chen, G. S. Huang, X. R. Qi, D. H. Zhang, and Y. S. Zhu, Phys. Rev. D **62**, 034003 (2000); R. L. Yang, R. G. Ping and H. Chen, Chin. Phys. Lett. **31**, 061301 (2014).
- [46] E. Richter-Was, Phys. Lett. B **303**, 163 (1993).
- [47] C. Langenbruch, Eur. Phys. J. C **82**, no.5, 393 (2022).
- [48] B. S. Zou and D. V. Bugg, Eur. Phys. J. A **16**, 537 (2003).
- [49] P. del Amo Sanchez *et al.* (BABAR Collaboration), Phys. Rev. D **83**, 052001 (2011).
- [50] M. Ablikim *et al.* (BESIII Collaboration), Phys. Rev. D **95**, 032002 (2017).
- [51] J. D. Jackson, N. Cimento **34**, 1644 (1964).
- [52] G. Bonvicini *et al.* (CLEO Collaboration), Phys. Rev. D **78**, 052001 (2011).
- [53] I. Adachi *et al.* (BABAR and BELLE Collaboration), Phys. Rev. D **98**, 112012 (2018).
- [54] M. Pivk and F. R. Le Diberder, Nucl. Instrum. Meth. A **555**, 356-369 (2005) doi:10.1016/j.nima.2005.08.106
- [55] R. G. Ping, Chin. Phys. C **32**, 599 (2008).
- [56] M. Ablikim *et al.* (BESIII Collaboration), Chin. Phys. C **44**, 040001 (2020).
- [57] B. C. Ke, J. Koponen, H. B. Li and Y. Zheng, Ann. Rev. Nucl. Part. Sci. **73**, 285-314 (2023).
- [58] H. B. Li and X. R. Lyu, Natl. Sci. Rev. **8**, no.11, nwab181 (2021).